

EI-Part: Explode for Completion and Implode for Refinement

Wanhu Sun^{1,3*} Zhongjin Luo^{1†} Heliang Zheng³ Jiahao Chang^{1,2} Chongjie Ye^{1,2}
 Huiang He³ Shengchu Zhao³ Rongfei Jia³ Xiaoguang Han^{1,2†}
¹SSE, CUHKSZ ²FNii-Shenzhen ³Math Magic



Figure 1. We present EI-Part, a novel framework designed to efficiently produce structurally coherent and semantically meaningful parts with fine-grained geometric details. Our work proposes an Explode-Implode strategy to fully utilize spatial resolution at different stages for meaningful part completion and geometric detail generation.

Abstract

Part-level 3D generation is crucial for various downstream applications, including gaming, film production, and industrial design. However, decomposing a 3D shape into geometrically plausible and meaningful components remains a significant challenge. Previous part-based generation methods often struggle to produce well-constructed parts, exhibiting either poor structural coherence, geometric implausibility, inaccuracy, or inefficiency. To address these challenges, we introduce EI-Part, a novel framework specifically designed

to generate high-quality 3D shapes with components, characterized by strong structural coherence, geometric plausibility, geometric fidelity, and generation efficiency. We propose utilizing distinct representations at different stages: an Explode state for part completion and an Implode state for geometry refinement. This strategy allows us to fully leverage spatial resolution, enabling flexible part completion and fine geometric details generation. To maintain structural coherence between parts, a self-attention mechanism is incorporated in both the exploded and imploded states, facilitating effective information perception and feature fusion among components during generation. Extensive experiments conducted on various benchmarks demonstrate that EI-Part efficiently yields semantically meaningful and

*Work done during internship at MathMagic.

†Corresponding authors: Z. Luo and X. Han.

structurally coherent parts with fine-grained geometric details, achieving state-of-the-art performance in part-level generation compared to existing methods. Project page: <https://cvhadessun.github.io/EI-Part/>

1. Introduction

3D content generation has become increasingly vital across various fields, including gaming, film production, and industrial design. Recent advancements in this area have been driven by the emergence of extensive 3D datasets [9, 10] and sophisticated generative models [27, 37, 46, 55]. However, despite these advancements, many current methods [7, 20–22, 53, 58] produce 3D assets in a monolithic form, lacking the nuanced part-level decomposition essential for detailed manipulation and editing. This limitation significantly hinders their ability to create complex assets that can be easily customized for various applications.

Within this landscape, part-based generation plays a critical role in the overall process of 3D content creation. To ensure that the generated parts meet downstream functionality, achieving high-quality part-level generation poses several essential criteria: 1) **Structural Coherence**. Maintaining structural coherence among parts is vital to ensure that the relationships and connections between different components are logical and consistent. 2) **Geometric Plausibility**. The generated parts must be geometrically plausible, meaning that each component should fit well within the overall structure and possess meaningful shapes and features that align with its intended function. 3) **Fidelity**. Achieving high fidelity in geometric details is essential for producing realistic outputs that accurately capture both visual realism and fine geometric characteristics of real-world objects. 4) **Efficiency**. Enhancing computational efficiency in both time and space is crucial for reducing the costs associated with part generation, thereby facilitating faster iterations and adjustments during the 3D design process. Coherence and plausibility are crucial for functional performance, while fidelity is essential for aesthetic appeal, and efficiency is important for cost reduction, all of which jointly contribute to effective 3D part generation.

Although several works [24, 42, 48, 51, 52, 56] have emerged to focus on 3D part generation, many of these efforts do not fully consider the aforementioned criteria, leading to failures to produce well-constructed parts. BANG [56] and PartPacker [42] embed all parts into either a single set or a dual set of latent codes, which constrains the representation capability of each part and consequently results in poor geometric details. HoloPart [51] enhances geometric details by representing each part as an independent set of latent codes and generating each individual part independently, but it neglects the relationships between parts, leading to poor structural coherence among them. PartCrafter [24] and

X-Part [48] enhance structural coherence by incorporating a cross-attention mechanism among part tokens during the generation process. However, their reliance on fixed-length part tokens is inflexible for parts with varying sizes, which results in inefficient resource allocation (limited capability to represent large components and wasted capacity for small components). OmniPart [52] improves representation efficiency by utilizing voxel-based representations, which adaptively allocate spatial resolution to each part and generate part shapes within each designated region defined by bounding boxes. However, assigning voxels in their consolidated state often leads to two issues: 1) overlapping voxels between parts, which would result in ambiguity during the completion process, and 2) can only occur within the limited active voxels confined by the bounding boxes, preventing any expansion beyond these boundaries. These two issues may jointly hinder its ability to produce meaningful parts. In conclusion, all existing methods struggle to produce well-constructed parts, exhibiting either poor structural coherence (e.g., HoloPart), geometric implausibility (e.g., OmniPart), inaccuracy (e.g., BANG, PartPacker), or inefficiency (e.g., PartCrafter, X-Part).

In this paper, we introduce EI-Part, a novel framework designed to generate well-constructed parts through an *Explode for Completion and Implode for Refinement* strategy. Our work meets the aforementioned criteria through two primary strategies: 1) *Exploding incomplete 3D parts to fully utilize spatial capacity for meaningful part generation, and 2) Imploding coarse part shapes to maximize spatial resolution for effectively capturing fine-grained geometric details*. Specifically, we first repurpose a multi-view diffusion model for mesh segmentation to obtain the initial incomplete 3D parts. Next, to enhance efficiency and geometric plausibility, we represent these incomplete parts as sparse voxels and apply an explosion strategy to complete the parts in a dispersed state. This explosion strategy not only avoids ambiguity caused by overlapping voxels between parts but also expands the resolution available for part completion, allowing for the generation of reasonable and meaningful components. Finally, to improve geometric fidelity, we propose reverting the exploded 3D voxels to an imploded state, fully utilizing spatial resolution to refine geometric details. Additionally, to maintain structural coherence between parts, we adopt a self-attention mechanism in both the exploded and imploded states, enabling information perception and feature fusion among components during shape completion and geometry refinement.

To evaluate the effectiveness of EI-Part, we conducted extensive experiments on various benchmarks. Our results demonstrate that EI-Part can efficiently generate semantically meaningful and structurally coherent parts with fine-grained geometries. Comparisons with existing approaches show that EI-Part achieves state-of-the-art performance in

part-level generation. In summary, the contributions of our work are as follows:

- We propose EI-Part, a novel framework dedicated to producing high-quality 3D shapes with well-constructed parts, characterized by strong structural coherence, geometric plausibility, accuracy, and efficiency.
- We introduce an Explode-Implode strategy to fully utilize spatial resolution at different stages: Explode for meaningful part completion and Implode for geometric details refinement.
- Extensive experiments demonstrate that our method achieves superior performance in part-level generation compared to state-of-the-art approaches.

2. Related Work

3D Object Generation. Traditionally, the limitations of data scale and computational resources have constrained 3D generation and reconstruction to specific categories [4, 28, 30, 32, 38, 44]. In the past few years, the emergence of large 3D datasets [9, 10], efficient representations [15, 19, 36, 39, 54], and advanced generative models [27, 37, 46, 55] has facilitated a significant evolution in 3D object generation, transitioning from category-specific approaches to open-world object generation.

As a pioneering effort, CLAY [55] integrates large-scale data with sophisticated transformer-based architectures for direct 3D generation. Subsequently, many works have aimed to enhance accuracy, efficiency, and controllability. TripoSG [21] leverages large-scale rectified flow transformers for high-fidelity 3D shape synthesis. HunYuan3D [58] employs scalable flow-based diffusion transformers alongside with high-quality datasets to create geometries that align with input conditions. TRELLIS [46] utilizes a voxel-based structured latent representation to achieve precise geometry generation in a coarse-to-fine manner. Hi3DGen [53] proposes a method to generate high-fidelity 3D geometry from images by utilizing normal maps as a bridge. Sparc3D [22] introduces a sparse deformable marching cubes representation for high-resolution generative modeling, facilitating the generation of fine-grained shape details. Furthermore, some recent works explore the generation of artist-like topologies and leverage autoregressive models to directly produce explicit faces [6, 14, 40, 45]. However, the aforementioned methods typically generate 3D objects as monolithic entities without part decomposition, which limits subsequent manipulation, editing and animation. Our work proposes a novel method for efficiently generating well-constructed parts, thereby facilitating downstream applications.

3D Part Segmentation. Traditional methods primarily extract high-level point features and predict per-point labels for 3D segmentation [34, 35, 57]. Most of these approaches rely on extensive annotations for supervised learning, which

limits them to category-specific segmentation and hinders their ability to generalize to open-world object scenarios. With the advent of 2D foundation models [3, 13, 17, 31], some methods have begun to lift 2D visual knowledge to 3D domains [41, 43, 47, 59]. While these approaches can generalize to open-world objects, their segmentation performance remains constrained, particularly in addressing self-occlusion scenarios.

In recent years, several works have aimed to leverage large-scale 3D datasets and advanced diffusion models to enhance the generalization of 3D segmentation. SAM-Part3D [50] introduces a scalable zero-shot 3D part segmentation approach that distills part-level 2D visual features into the 3D domain using a trained 3D backbone for multi-granularity segmentation. PartField [26] proposes a feed-forward framework that learns a part-based 3D feature field through contrastive learning and performs part decomposition via clustering. P3-SAM [29] presents a 3D-native point-promptable part segmentation model that integrates point features across different levels, leveraging point-wise features for 3D part segmentation. However, due to limitations in 3D resolution, these methods often yield unsatisfactory segmentation results and struggle to produce clear boundaries. In this work, we propose a multi-view diffusion model for part segmentation to achieve robust segmentation results with well-defined boundaries.

3D Part Generation. Beyond 3D part segmentation, 3D part generation seeks to create complete, geometrically plausible, and meaningful components that fulfill practical requirements in both aesthetic appeal and intended functionality. However, existing methods struggle to produce well-constructed parts. PartGen [5] reconstructs components from multi-view segmented results independently, resulting in poor structural coherence.

BANG [56] formulates part generation as an object explosion process but embeds parts into a single set of latent codes, leading to insufficient geometric detail. Similarly, the dual latent codes used in PartPacker [42] restrict its ability to capture fine geometric details. HoloPart [51] generates each part independently, neglecting the interrelationships between parts and thereby diminishing structural coherence. To enhance coherence, PartCrafter [24] incorporates cross-attention mechanisms between parts, while X-Part [48] introduces an inter-part attention module. However, their reliance on fixed-length part tokens is inflexible for addressing parts of varying sizes, resulting in inefficient resource allocation. OmniPart [52] employs voxel-based representations to adaptively allocate space for components of different sizes. Nonetheless, the use of bounding boxes not only restricts the available resolution for completion but also leads to overlapping voxels between parts, thereby hindering the generation of meaningful components.

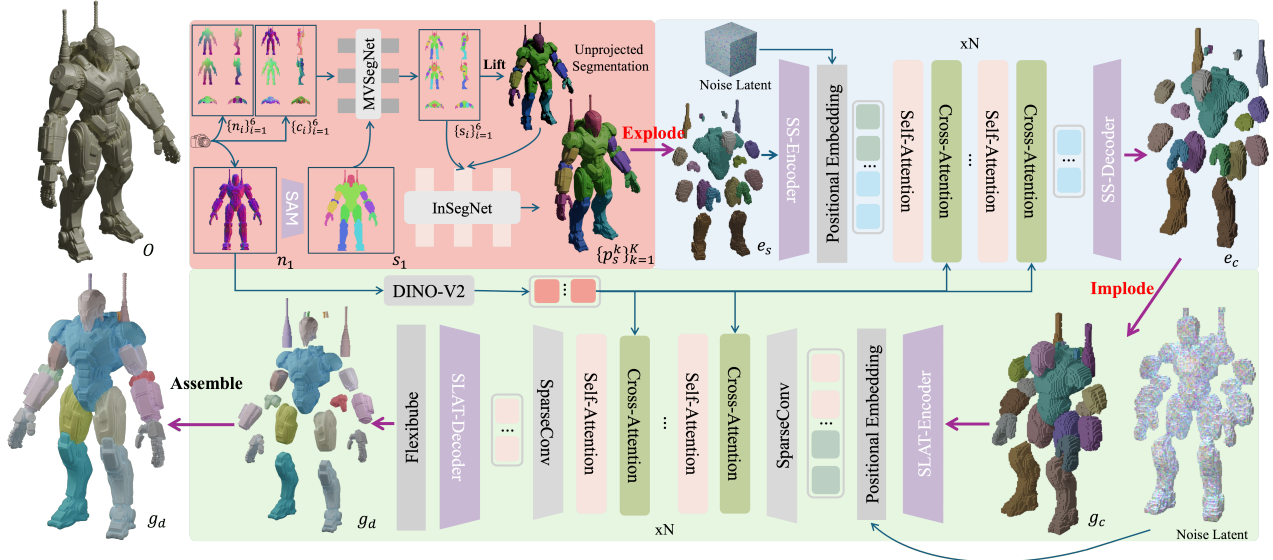


Figure 2. The pipeline of our proposed EI-Part. Given an input 3D shape O , we first obtain its normal map $\{n_i\}_{i=1}^6$ and canonical coordinate maps (CCMs) $\{c_i\}_{i=1}^6$ from six views. We then perform frontal segmentation using SAM and employ MVSegNet to achieve multi-view consistent segmentations. These segmentations are lifted to 3D to create an initial part segmentation, which is subsequently inpainted by InSegNet to produce accurate 3D segmented shapes $\{p_s^k\}_{k=1}^K$. The segmented result is exploded into discrete 3D voxels, enabling us to perform conditional diffusion completion to generate geometrically plausible and complete part structures e_c . Next, the exploded complete parts are imploded back to a compact state for conditional diffusion refinement, capturing fine-level details g_d . Thanks to the utilization of the exploded-imploded strategy, we fully utilize spatial resolution at different stages, enhancing the accuracy of part completion and surface details. As a result, the 3D shapes g_d generated by our method exhibit individual, structurally consistent, and geometrically plausible part shapes with fine-grained geometric details.

In this paper, we propose a novel framework designed to produce high-quality 3D shapes with well-constructed parts, achieving strong structural coherence, geometric plausibility, accuracy, and efficiency.

3. Method

The overview of our method is shown in Fig. 2. Given an input 3D shape, we first obtain its normal map and canonical coordinate maps from six views. We then perform frontal segmentation using SAM and employ MVSegNet to achieve multi-view consistent segmentations. These segmentations are lifted to 3D to create an initial part segmentation, which is subsequently inpainted by InSegNet to produce accurate 3D segmented shapes. The segmented result is exploded into discrete 3D voxels, enabling us to perform conditional diffusion completion to generate geometrically plausible and complete part structures. Next, the exploded complete parts are imploded back to a compact state for conditional diffusion refinement, capturing fine-level details. Thanks to the utilization of the exploded-imploded strategy, we fully utilize spatial resolution at different stages, enhancing the accuracy of part completion and surface details. As a result, the 3D shapes generated by our method exhibit individual, structurally consistent, and geometrically plausible part shapes

with fine-grained geometric details.

3.1. Diffusion Part Segmentation

Given an input 3D shape, we first decompose it into semantically meaningful parts. Inspired by texturing techniques [2, 23, 49, 58], we adopt a two-stage diffusion-based framework for robust 3D part segmentation. This framework first generates multiview segmentations and then propagates this semantic knowledge into 3D space to learn a continuous semantic field.

To be specific, for an input shape O , we render its normal maps $\{n_i\}_{i=1}^6$ and canonical coordinate maps (CCMs) $\{c_i\}_{i=1}^6$ from six orthographic views. We then obtain a frontal-view segmentation s_1 using SAM [17]. The normal maps $\{n_i\}_{i=1}^6$, CCMs $\{c_i\}_{i=1}^6$, and frontal segmentation s_1 serve as input for our multiview segmentation diffusion model (MVSegNet) to generate consistent segmentations across six viewpoints. A straightforward approach for obtaining 3D segmentation is to directly unproject the multiview segmentations onto the 3D shape. However, this method would lead to inaccuracies in occluded and unseen regions. To address this, we utilize an inpainting model (InSegNet) to refine part segmentation. Taking the multiview segmentations and the unprojected 3D segmentations as input, InSeg-

Net extracts semantic features (f_{2D}, f_{3D}) from both 2D and 3D segmentation, subsequently learning a continuous 3D semantic field. Formally, for each point x on the 3D surface, we can query its semantic color from the learned field via $\hat{S}(x) = \text{InSegNet}(x, f_{2D}, f_{3D})$. The InSegNet is trained by minimizing the following loss function [23, 38],

$$\mathcal{L}_{seg} = \frac{1}{n} \sum_{i=1}^n |\hat{S}(x_i) - S(x_i)|, \quad (1)$$

where $\hat{S}(\cdot)$ denotes the predicted semantic RGB color and $S(\cdot)$ represents the ground truth. x_i denotes the i -th sampled point, and n is the number of sampled points. Given the learned semantic field, we densely sample points from O and query their semantic colors, obtaining K globally consistent and seamless 3D parts $\{p_s^k\}_{k=1}^K$.

3.2. Explode for Completion

Although the 3D segmentation outputs individual parts, their incompleteness limits their applicability in downstream tasks. To achieve geometrically plausible and complete part structures for their intended functionality, we propose to explode the 3D segmented points into a dispersed state, thereby extending the available spatial resolution for better part completion. Compared to OmniPart [52], which is limited to performing completion within active voxels, our part completion strategy fully leverages spatial resolution to expand available completion extents.

Specifically, we convert $\{p_s^k\}_{k=1}^K$ into explicit segmented voxels $\{v_s^k\}_{k=1}^K$ and utilize a sparse structured representation for subsequent part generation. The voxel-based representation enables us to flexibly represent parts of varying sizes, with larger parts occupying more voxels and smaller parts fewer, thereby enhancing spatial efficiency. Inspired by [56], we employ explosion vector optimization to explode $\{v_s^k\}_{k=1}^K$ radially outward. We compute the axis-aligned bounding boxes for each part v_s^k and optimize a translation vector to diffuse $\{v_s^k\}_{k=1}^K$ from a converged state into a dispersed state $e_s = \text{Explode}(\{v_s^k\}_{k=1}^K)$. The translation directions $\{u_k\}_{k=1}^K$ and distances $\{\mathbf{d}_k\}_{k=1}^K$ are recorded to facilitate subsequent implosion. Let e_c be complete parts, given the frontal normal map n_1 and the exploded part voxels e_s as input, we model the conditional part completion as a structured diffusion process $p_\theta(e_c | e_s, n_1)$. Thanks to the utilization of exploded voxels, structural information perception between part voxels, as well as cross-modal feature fusion between the normal map and the voxels, can be integrated in a highly efficient manner [1] during the completion process:

$$\mathcal{F}_E = \text{CrossAttn}(D_n, \text{SelfAttn}(\text{Concat}(E_s, Z_t))). \quad (2)$$

These operations are performed in latent feature space. We obtain 2D tokens D_n of the normal map using DINOv2 [31]

and 3D voxel-based conditional latent features E_s of the incomplete parts via the SS-VAE encoder [46] to generate the target structured latents E_c of the complete parts. Z_t denotes the latent noise at the t -th step. This advantageous fusion of different features significantly enhances both the structural coherence and accuracy of the resulting complete parts. Our conditional completion is formulated as a rectified flow-based diffusion process with DiT [33] and trained using Conditional Flow Matching (CFM) [25]:

$$\mathcal{L}_{CFM}(\theta) = \mathbb{E}_{\mathbf{x}_0, t, \epsilon} \|\mathbf{v}_\theta(\mathbf{x}, t) - (\epsilon - \mathbf{x}_0)\|_2^2. \quad (3)$$

3.3. Implode for Refinement

In the completion stage, we represent incomplete part voxels in an exploded state to generate complete part structures. This process is designed to fully utilize spatial resolution to produce complete, structurally coherent, and geometrically plausible parts while disregarding fine-level geometric details. Consequently, we propose to implode the complete exploded coarse part structures into an imploded state, thereby maximizing spatial resolution again to capture fine-grained geometric details.

In particular, the generated structured latents E_c is decoded to obtain the complete part voxels e_c . To implode e_c into a more compact spatial distribution, we sort all part voxels by their distance from the center and adjust their positions. Instead of moving parts along the opposite direction $\{-u_k\}_{k=1}^K$ of the explosion by the exploded distance $\{\mathbf{d}_k\}_{k=1}^K$ via $m_k' = m_k - \mathbf{d}_k \cdot u_k$, we propose to update the positions $\{m_k\}_{k=1}^K$ of the parts iteratively by,

$$m_k^{j+1} = m_k^j - \alpha \cdot u_k, \quad (4)$$

where α is the step size that determines how quickly the parts approach the center, while j denotes the j -th iteration. This iterative process would stop when collisions occur among the parts. After obtaining the imploded complete voxels g_c , we model the geometric detail refinement as a conditional generative diffusion process. Let g_d represent high-fidelity parts with fine-grained geometric details. Given the frontal normal map n_1 , the exploded and imploded complete voxels (e_c, g_c), the refinement process is formulated as $p_\theta(g_d | g_c, e_c, n_1)$. Similarly, we integrate structural information and cross-modal features by:

$$\mathcal{F}_I = \text{CrossAttn}(D_n, \text{SelfAttn}(\text{Concat}(G_c, E_c, Z_t))). \quad (5)$$

The refinement process is also executed in structured latent space, and the model is trained using the CFM loss as described in Eq. 3. The 2D tokens D_n are also extracted using DINOv2. In contrast to the completion stage, we utilize a more powerful VAE, Sparc3D [22], to extract voxel-based conditional features from (G_c, E_c) and decode the target part geometries g_d from the generated structured latents G_d .

Table 1. Quantitative comparison between our method and state-of-the-art methods in part generation. Our method achieves the best performance across all evaluation metrics, demonstrating superior shape fidelity and geometric accuracy. Note that BANG is a commercial product with no open-source code available, making quantitative comparison infeasible.

| Method | Voxel IOU \uparrow | CD \downarrow | Voxel F-Score 0.01 \uparrow | F-Score 0.1 \uparrow | F-Score 0.05 \uparrow | F-Score 0.01 \uparrow |
|------------------|----------------------|-----------------|-------------------------------|------------------------|-------------------------|-------------------------|
| PartPacker [42] | 0.2586 | 0.1273 | 0.3768 | 0.8199 | 0.6428 | 0.2435 |
| PartCrafter [24] | 0.0742 | 0.3474 | 0.1316 | 0.4429 | 0.2801 | 0.0749 |
| HoloPart [51] | 0.6106 | 0.0431 | 0.7374 | 0.9557 | 0.9402 | 0.6400 |
| X-Part [48] | 0.7478 | 0.0599 | 0.8413 | 0.9256 | 0.9087 | 0.7923 |
| OmniPart [52] | 0.2861 | 0.1431 | 0.4007 | 0.7911 | 0.6516 | 0.2644 |
| Ours | 0.7981 | 0.0194 | 0.8452 | 0.9910 | 0.9742 | 0.8129 |



Figure 3. Qualitative comparison between ours and the state of the arts. For each row, the input model (a) is followed by the parts generated by (b) BANG [56], (c) HoloPart [51], (d) X-Part [48], (e) OmniPart [52] and (f) our method. Our method demonstrates proficiency in generating high-quality 3D shapes with well-defined parts, achieving notable performance in structural coherence, geometric plausibility, fidelity, and efficiency. Please refer to our supplementary materials for a qualitative comparison with additional methods (e.g., PartPacker and PartCrafter).

As a result, g_d contains individual, structurally consistent and geometrically plausible part shapes with fine-grained geometric details.

4. Experiments

Data Preparation. We collected datasets from well-known 3D object datasets including Objaverse [9], Objaverse-XL [10], ABO [8], 3D-FUTURE [12] and HSSD [16]. The GLB files in these datasets are 3D models



Figure 4. Qualitative comparison between our method and the state of the art, where all methods share the segmentation results of ours. Each row presents the input model (a), followed by (b) our segmentation, and the parts generated by (c) HoloPart [51], (d) X-Part [48], (e) OmniPart [52] and (f) our method.

created by professionals, some of which inherently possess individual parts. We adopt the following strategy to obtain our data: 1) Filtering. We establish a threshold of 20 parts to construct the initial dataset, filtering out GLB files with excessive part counts. 2) Processing. For GLB files in the initial dataset, we further split the files based on connectivity, resulting in numerous independent sub-meshes. When the number of sub-meshes exceeds 20, we sort them by face count, surface area, and a weighted bounding box value. The n smallest sub-meshes are then merged into larger part meshes based on collision proximity (or the nearest bbox if no collision exists) to construct the final GLB.

Implementation details. We trained our model utilizing the collected data. Both MVSegNet and InSegNet were optimized using the Adam optimizer, with a learning rate of 3×10^{-4} , over a duration of 4 days on 32 GPUs. For the exploded completion model, we employed the Adam optimizer with a learning rate of 1×10^{-4} , incorporating gradient clipping with a maximum norm of 1.0 to enhance training stability. This training was conducted on 64 GPUs for a total of two weeks (14 days), with a probability of 0.3 for introducing zero conditions to further improve robustness. The imploded refinement model was fine-tuned using the Adam optimizer at a learning rate of 1×10^{-4} on the Sparc3D checkpoint, with a training duration of 6 days on 64 GPUs. Please refer to the supplementary materials for additional implementation details.

Evaluation Metrics. We utilize Chamfer Distance (CD), Intersection over Union (IoU), and F-Score to assess the accuracy and completeness of the generated geometry. CD, IoU, and F-Score are evaluated by sampling 100,000 points from the 3D outputs, with all object points normalized to the range of $[-1, 1]^3$. When calculating the F-Score, the radius is set to 0.1, 0.05, and 0.01, while the Voxel F-Score is set to 0.01. Voxel F-Score and Voxel IoU are computed using 3D voxels. The evaluation is conducted using PartVerse [11].

Comparison with Baseline Methods. To validate the effectiveness of our approach, we compare it against state-of-the-art part generation models, both quantitatively and qualitatively: BANG [56], HoloPart [51], X-Part [48], and OmniPart [52]. Tab. 1 shows the quantitative comparisons. Our proposed method achieves the best scores against the baselines. Fig. 3 provides qualitative results of 3D part generation. Please refer to our supplementary materials for a qualitative comparison with additional methods (e.g., PartPacker [42] and PartCrafter [24]). As observed, BANG [56] struggles to capture fine geometric details that align with the input model. This issue arises from its practice of embedding all components into a single set of latent tokens, which restricts the representational capacity of each individual part and ultimately leads to inaccuracies in geometric details. The inaccurate 3D part segmentation employed in HoloPart [51], X-Part [48], and OmniPart [52] results in numerous implausible parts. HoloPart [51] enhances geometric details by representing each part as an independent set

of latent codes and generating them individually; however, it neglects the interrelationships between parts, resulting in unnatural completion outcomes akin to merely filling a hole, thereby leading to poor structural coherence. Meanwhile, X-Part [48] improves structural coherence through a cross-attention mechanism among parts, yet its reliance on fixed-length part tokens is inflexible for components of varying sizes. This limitation results in inefficient resource allocation, yielding insufficient capability to represent larger components while wasting capacity on smaller ones. While OmniPart [52] utilizes voxel-based representations to adaptively allocate spatial resolution to different parts, it only supports completion within active voxels, thereby restricting the available spatial extents for completion. This limitation can lead to implausible part geometry and decreased geometric fidelity. Our method demonstrates proficiency in generating high-quality 3D shapes with well-defined parts, achieving notable performance in structural coherence, geometric plausibility, geometric fidelity, and efficiency. Notably, the Explode-Implode strategy enables our approach to robustly perform meaningful part completion and fine-level geometric generation. To evaluate the impact of our proposed Explode-Implode generation framework, we conduct a comparison with segmentation-based methods using the same 3D segmentation (our segmentation) as input. Segmentation-based methods refer to those approaches that take 3D segmentation as input for part generation, including HoloPart, X-Part, OmniPart and our EI-Part. As shown in Fig 4, despite using the same segmentation, our method still demonstrates superior performance in both geometric plausibility and fidelity.



Figure 5. Qualitative comparison between our method and the alternative strategies. The input is the same segmentation.

Ablation Study on Explode and Implode. To demonstrate the necessity of our Explode and Implode strategy, we conduct an ablation study in the following scenarios: 1) without both explosion and implosion; 2) with explosion but without implosion; and 3) with both components (i.e., our

proposed method). As illustrated in Fig. 5, the results generated without explosion yield implausible part geometry, while the results generated without implosion fail to capture fine geometric details. The corresponding quantitative evaluations can be found in the supplementary material.

Ablation Study on Part Segmentation. To highlight the importance of our part segmentation model, we conduct an ablation study comparing our model with alternative methods (i.e., PartField [26] and P3-SAM [29]). As shown in Fig. 6, the results produced by our method exhibit more accurate and meaningful segmentation.

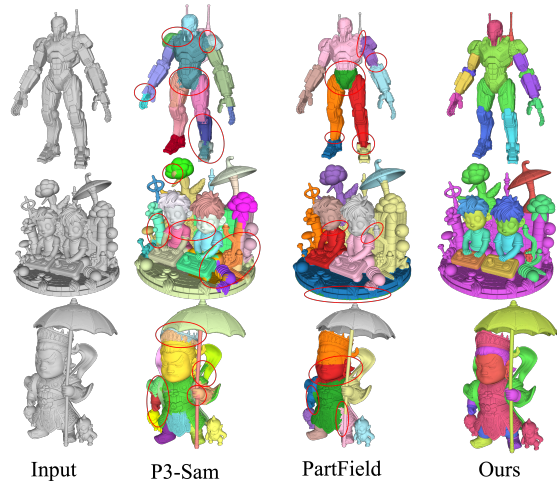


Figure 6. Qualitative comparison between our segmentation method and the alternative methods.

5. Conclusion

Part-level generation remains a significant challenge in 3D content creation, as it requires balancing structural coherence and geometric plausibility while ensuring accuracy and computational efficiency. In this work, we present EI-Part, a novel framework that addresses the critical challenges of 3D part generation through a novel Explode-Implode strategy, enabling the production of high-quality 3D shapes with well-constructed parts. The explosion phase allows for the comprehensive utilization of spatial capacity, facilitating meaningful part generation while mitigating issues related to overlapping voxels. Subsequently, the implosion phase maximizes spatial resolution, enabling the capture of fine-grained geometric details essential for realistic 3D assets. Our extensive experiments across various benchmarks demonstrate that EI-Part outperforms existing state-of-the-art methods in part-level generation, yielding semantically meaningful and structurally coherent parts. The results underscore the effectiveness of our framework in producing high-quality

3D parts, thereby advancing the field of 3D content generation. Future work will explore further enhancements to our method by integrating physical principles into the generation process to better address complex scenarios that require high physical accuracy.

References

- [1] Stephen Batifol, Andreas Blattmann, Frederic Boesel, Saksham Consul, Cyril Diagne, Tim Dockhorn, Jack English, Zion English, Patrick Esser, Sumith Kulal, et al. Flux. 1 kontext: Flow matching for in-context image generation and editing in latent space. *arXiv e-prints*, pages arXiv-2506, 2025. 5, 1
- [2] Raphael Bensadoun, Yanir Kleiman, Idan Azuri, Omri Harosh, Andrea Vedaldi, Natalia Neverova, and Oran Gafni. Meta 3d texturegen: Fast and consistent texture generation for 3d objects. *arXiv preprint arXiv:2407.02430*, 2024. 4
- [3] Mathilde Caron, Hugo Touvron, Ishan Misra, Hervé Jégou, Julien Mairal, Piotr Bojanowski, and Armand Joulin. Emerging properties in self-supervised vision transformers. In *Proceedings of the International Conference on Computer Vision (ICCV)*, 2021. 3
- [4] Angel X Chang, Thomas Funkhouser, Leonidas Guibas, Pat Hanrahan, Qixing Huang, Zimo Li, Silvio Savarese, Manolis Savva, Shuran Song, Hao Su, et al. Shapenet: An information-rich 3d model repository. *arXiv preprint arXiv:1512.03012*, 2015. 3
- [5] Minghao Chen, Roman Shapovalov, Iro Laina, Tom Monnier, Jianyuan Wang, David Novotny, and Andrea Vedaldi. Partgen: Part-level 3d generation and reconstruction with multi-view diffusion models. *arXiv preprint arXiv:2412.18608*, 2024. 3
- [6] Yiwen Chen, Tong He, Di Huang, Weicai Ye, Sijin Chen, Jiayang Tang, Xin Chen, Zhongang Cai, Lei Yang, Gang Yu, et al. Meshanything: Artist-created mesh generation with autoregressive transformers. *arXiv preprint arXiv:2406.10163*, 2024. 3
- [7] Yiwen Chen, Zhihao Li, Yikai Wang, Hu Zhang, Qin Li, Chi Zhang, and Guosheng Lin. Ultra3d: Efficient and high-fidelity 3d generation with part attention. *arXiv preprint arXiv:2507.17745*, 2025. 2
- [8] Jasmine Collins, Shubham Goel, Kenan Deng, Achleshwar Luthra, Leon Xu, Erhan Gundogdu, Xi Zhang, Tomas F Yago Vicente, Thomas Dideriksen, Himanshu Arora, et al. Abo: Dataset and benchmarks for real-world 3d object understanding. In *Proceedings of the IEEE/CVF conference on computer vision and pattern recognition*, pages 21126–21136, 2022. 6
- [9] Matt Deitke, Dustin Schwenk, Jordi Salvador, Luca Weihs, Oscar Michel, Eli VanderBilt, Ludwig Schmidt, Kiana Ehsani, Aniruddha Kembhavi, and Ali Farhadi. Objaverse: A universe of annotated 3d objects. *arXiv preprint arXiv:2212.08051*, 2022. 2, 3, 6
- [10] Matt Deitke, Ruoshi Liu, Matthew Wallingford, Huong Ngo, Oscar Michel, Aditya Kusupati, Alan Fan, Christian Laforte, Vikram Voleti, Samir Yitzhak Gadre, Eli VanderBilt, Aniruddha Kembhavi, Carl Vondrick, Georgia Gkioxari, Kiana Ehsani, Ludwig Schmidt, and Ali Farhadi. Objaverse-xl: A universe of 10m+ 3d objects. *arXiv preprint arXiv:2307.05663*, 2023. 2, 3, 6
- [11] Shaocong Dong, Lihe Ding, Xiao Chen, Yaokun Li, Yuxin WANG, Yucheng Wang, Qi WANG, Jaehyeok Kim, Chenjian Gao, Zhanpeng Huang, Zibin Wang, Tianfan Xue, and Dan Xu. From one to more: Contextual part latents for 3d generation. 2025. 7
- [12] Huan Fu, Rongfei Jia, Lin Gao, Mingming Gong, Binqiang Zhao, Steve Maybank, and Dacheng Tao. 3d-future: 3d furniture shape with texture. *International Journal of Computer Vision*, 129(12):3313–3337, 2021. 6
- [13] Markus Hafner, Maria Katsantoni, Tino Köster, James Marks, Joyita Mukherjee, Dorothee Staiger, Jernej Ule, and Mihaela Zavolan. Clip and complementary methods. *Nature Reviews Methods Primers*, 1(1):20, 2021. 3
- [14] Zekun Hao, David W Romero, Tsung-Yi Lin, and Ming-Yu Liu. Meshtron: High-fidelity, artist-like 3d mesh generation at scale. *arXiv preprint arXiv:2412.09548*, 2024. 3
- [15] Bernhard Kerbl, Georgios Kopanas, Thomas Leimkühler, and George Drettakis. 3d gaussian splatting for real-time radiance field rendering. *ACM Trans. Graph.*, 42(4):139–1, 2023. 3
- [16] Mukul Khanna, Yongsan Mao, Hanxiao Jiang, Sanjay Haresh, Brennan Shacklett, Dhruv Batra, Alexander Clegg, Eric Undersander, Angel X Chang, and Manolis Savva. Habitat synthetic scenes dataset (hssd-200): An analysis of 3d scene scale and realism tradeoffs for objectgoal navigation. In *Proceedings of the IEEE/CVF Conference on Computer Vision and Pattern Recognition*, pages 16384–16393, 2024. 6
- [17] Alexander Kirillov, Eric Mintun, Nikhila Ravi, Hanzi Mao, Chloe Rolland, Laura Gustafson, Tete Xiao, Spencer Whitehead, Alexander C. Berg, Wan-Yen Lo, Piotr Dollár, and Ross Girshick. Segment anything. *arXiv:2304.02643*, 2023. 3, 4
- [18] Black Forest Labs. Flux. <https://github.com/black-forest-labs/flux>, 2024. 1
- [19] Muheng Li, Yueqi Duan, Jie Zhou, and Jiwen Lu. Diffusion-sdf: Text-to-shape via voxelized diffusion. In *Proceedings of the IEEE/CVF conference on computer vision and pattern recognition*, pages 12642–12651, 2023. 3
- [20] Weiyu Li, Jiarui Liu, Hongyu Yan, Rui Chen, Yixun Liang, Xuelin Chen, Ping Tan, and Xiaoxiao Long. Craftsman3d: High-fidelity mesh generation with 3d native generation and interactive geometry refiner. *arXiv preprint arXiv:2405.14979*, 2024. 2
- [21] Yanguang Li, Zi-Xin Zou, Zexiang Liu, Dehu Wang, Yuan Liang, Zhipeng Yu, Xingchao Liu, Yuan-Chen Guo, Ding Liang, Wanli Ouyang, et al. Triposg: High-fidelity 3d shape synthesis using large-scale rectified flow models. *arXiv preprint arXiv:2502.06608*, 2025. 3
- [22] Zhihao Li, Yufei Wang, Heliang Zheng, Yihao Luo, and Bihan Wen. Sparc3d: Sparse representation and construction for high-resolution 3d shapes modeling. *arXiv preprint arXiv:2505.14521*, 2025. 2, 3, 5, 1
- [23] Yixun Liang, Kunming Luo, Xiao Chen, Rui Chen, Hongyu Yan, Weiyu Li, Jiarui Liu, and Ping Tan. Unitex: Universal high fidelity generative texturing for 3d shapes. *arXiv preprint arXiv:2505.23253*, 2025. 4, 5, 1
- [24] Yuchen Lin, Chenguo Lin, Panwang Pan, Honglei Yan, Yiqiang Feng, Yadong Mu, and Katerina Fragkiadaki. Partcrafter: Structured 3d mesh generation via compositional latent diffusion transformers. *arXiv preprint arXiv:2506.05573*, 2025. 2, 3, 6, 7, 1
- [25] Yaron Lipman, Ricky TQ Chen, Heli Ben-Hamu, Maximilian Nickel, and Matt Le. Flow matching for generative modeling. *arXiv preprint arXiv:2210.02747*, 2022. 5

- [26] Minghua Liu, Mikaela Angelina Uy, Donglai Xiang, Hao Su, Sanja Fidler, Nicholas Sharp, and Jun Gao. Partfield: Learning 3d feature fields for part segmentation and beyond. In *Proceedings of the IEEE/CVF International Conference on Computer Vision*, pages 9704–9715, 2025. 3, 8
- [27] Ruoshi Liu, Rundi Wu, Basile Van Hoorick, Pavel Tokmakov, Sergey Zakharov, and Carl Vondrick. Zero-1-to-3: Zero-shot one image to 3d object. In *Proceedings of the IEEE/CVF international conference on computer vision*, pages 9298–9309, 2023. 2, 3
- [28] Zhongjin Luo, Dong Du, Heming Zhu, Yizhou Yu, Hongbo Fu, and Xiaoguang Han. Sketchmetaface: A learning-based sketching interface for high-fidelity 3d character face modeling. *IEEE Transactions on Visualization and Computer Graphics*, 30(8):5260–5275, 2023. 3
- [29] Changfeng Ma, Yang Li, Xinhao Yan, Jiachen Xu, Yunhan Yang, Chunshi Wang, Zibo Zhao, Yanwen Guo, Zhuo Chen, and Chunchao Guo. P3-sam: Native 3d part segmentation. *arXiv preprint arXiv:2509.06784*, 2025. 3, 8
- [30] Lars Mescheder, Michael Oechsle, Michael Niemeyer, Sebastian Nowozin, and Andreas Geiger. Occupancy networks: Learning 3d reconstruction in function space. In *Proceedings of the IEEE/CVF conference on computer vision and pattern recognition*, pages 4460–4470, 2019. 3
- [31] Maxime Oquab, Timothée Darcet, Théo Moutakanni, Huy Vo, Marc Szafraniec, Vasil Khalidov, Pierre Fernandez, Daniel Haziza, Francisco Massa, Alaaeldin El-Nouby, et al. Dinov2: Learning robust visual features without supervision. *arXiv preprint arXiv:2304.07193*, 2023. 3, 5
- [32] Jeong Joon Park, Peter Florence, Julian Straub, Richard Newcombe, and Steven Lovegrove. Deepsdf: Learning continuous signed distance functions for shape representation. In *Proceedings of the IEEE/CVF conference on computer vision and pattern recognition*, pages 165–174, 2019. 3
- [33] William Peebles and Saining Xie. Scalable diffusion models with transformers. In *Proceedings of the IEEE/CVF international conference on computer vision*, pages 4195–4205, 2023. 5
- [34] Charles R Qi, Hao Su, Kaichun Mo, and Leonidas J Guibas. Pointnet: Deep learning on point sets for 3d classification and segmentation. In *Proceedings of the IEEE conference on computer vision and pattern recognition*, pages 652–660, 2017. 3
- [35] Charles Ruizhongtai Qi, Li Yi, Hao Su, and Leonidas J Guibas. Pointnet++: Deep hierarchical feature learning on point sets in a metric space. *Advances in neural information processing systems*, 30, 2017. 3
- [36] Xuanchi Ren, Jiahui Huang, Xiaohui Zeng, Ken Museth, Sanja Fidler, and Francis Williams. Xcube: Large-scale 3d generative modeling using sparse voxel hierarchies. In *Proceedings of the IEEE/CVF conference on computer vision and pattern recognition*, pages 4209–4219, 2024. 3
- [37] Robin Rombach, Andreas Blattmann, Dominik Lorenz, Patrick Esser, and Björn Ommer. High-resolution image synthesis with latent diffusion models. In *Proceedings of the IEEE/CVF conference on computer vision and pattern recognition*, pages 10684–10695, 2022. 2, 3
- [38] Shunsuke Saito, Zeng Huang, Ryota Natsume, Shigeo Morishima, Angjoo Kanazawa, and Hao Li. Pifu: Pixel-aligned implicit function for high-resolution clothed human digitization. In *Proceedings of the IEEE/CVF international conference on computer vision*, pages 2304–2314, 2019. 3, 5
- [39] J Ryan Shue, Eric Ryan Chan, Ryan Po, Zachary Ankner, Jiajun Wu, and Gordon Wetzstein. 3d neural field generation using triplane diffusion. In *Proceedings of the IEEE/CVF Conference on Computer Vision and Pattern Recognition*, pages 20875–20886, 2023. 3
- [40] Yawar Siddiqui, Antonio Alliegro, Alexey Artemov, Tatiana Tommasi, Daniele Sirigatti, Vladislav Rosov, Angela Dai, and Matthias Nießner. Meshgpt: Generating triangle meshes with decoder-only transformers. In *Proceedings of the IEEE/CVF conference on computer vision and pattern recognition*, pages 19615–19625, 2024. 3
- [41] George Tang, William Zhao, Logan Ford, David Benhaim, and Paul Zhang. Segment any mesh: Zero-shot mesh part segmentation via lifting segment anything 2 to 3d. *arXiv e-prints*, pages arXiv–2408, 2024. 3
- [42] Jiaxiang Tang, Ruijie Lu, Zhaoshuo Li, Zekun Hao, Xuan Li, Fangyin Wei, Shuran Song, Gang Zeng, Ming-Yu Liu, and Tsung-Yi Lin. Efficient part-level 3d object generation via dual volume packing. *arXiv preprint arXiv:2506.09980*, 2025. 2, 3, 6, 7, 1
- [43] Ardian Umam, Cheng-Kun Yang, Min-Hung Chen, Jen-Hui Chuang, and Yen-Yu Lin. Partdistill: 3d shape part segmentation by vision-language model distillation. In *IEEE/CVF International Conference on Computer Vision (CVPR)*, 2024. 3
- [44] Nanyang Wang, Yinda Zhang, Zhuwen Li, Yanwei Fu, Wei Liu, and Yu-Gang Jiang. Pixel2mesh: Generating 3d mesh models from single rgb images. In *Proceedings of the European conference on computer vision (ECCV)*, pages 52–67, 2018. 3
- [45] Yuxuan Wang, Xuanyu Yi, Haohan Weng, Qingshan Xu, Xiaokang Wei, Xianghui Yang, Chunchao Guo, Long Chen, and Hanwang Zhang. Nautilus: Locality-aware autoencoder for scalable mesh generation. *arXiv preprint arXiv:2501.14317*, 2025. 3
- [46] Jianfeng Xiang, Zelong Lv, Sicheng Xu, Yu Deng, Ruicheng Wang, Bowen Zhang, Dong Chen, Xin Tong, and Jiaolong Yang. Structured 3d latents for scalable and versatile 3d generation. In *Proceedings of the Computer Vision and Pattern Recognition Conference*, pages 21469–21480, 2025. 2, 3, 5, 1
- [47] Mutian Xu, Xingyilang Yin, Lingteng Qiu, Yang Liu, Xin Tong, and Xiaoguang Han. Sampro3d: Locating sam prompts in 3d for zero-shot instance segmentation. In *International Conference on 3D Vision (3DV)*, 2025. 3
- [48] Xinhao Yan, Jiachen Xu, Yang Li, Changfeng Ma, Yunhan Yang, Chunshi Wang, Zibo Zhao, Zeqiang Lai, Yunfei Zhao, Zhuo Chen, et al. X-part: high fidelity and structure coherent shape decomposition. *arXiv preprint arXiv:2509.08643*, 2025. 2, 3, 6, 7, 8, 1
- [49] Jiayu Yang, Taizhang Shang, Weixuan Sun, Xibin Song, Ziang Cheng, Senbo Wang, Shenzhou Chen, Weizhe Liu, Hongdong Li, and Pan Ji. Pandora3d: A comprehensive

- framework for high-quality 3d shape and texture generation. *arXiv preprint arXiv:2502.14247*, 2025. 4
- [50] Yunhan Yang, Yukun Huang, Yuan-Chen Guo, Liangjun Lu, Xiaoyang Wu, Edmund Y Lam, Yan-Pei Cao, and Xihui Liu. Sampart3d: Segment any part in 3d objects. *arXiv preprint arXiv:2411.07184*, 2024. 3
- [51] Yunhan Yang, Yuan-Chen Guo, Yukun Huang, Zi-Xin Zou, Zhipeng Yu, Yangguang Li, Yan-Pei Cao, and Xihui Liu. Holopart: Generative 3d part amodal segmentation. *arXiv preprint arXiv:2504.07943*, 2025. 2, 3, 6, 7, 1
- [52] Yunhan Yang, Yufan Zhou, Yuan-Chen Guo, Zi-Xin Zou, Yukun Huang, Ying-Tian Liu, Hao Xu, Ding Liang, Yan-Pei Cao, and Xihui Liu. Omnipart: Part-aware 3d generation with semantic decoupling and structural cohesion. *arXiv preprint arXiv:2507.06165*, 2025. 2, 3, 5, 6, 7, 8, 1
- [53] Chongjie Ye, Yushuang Wu, Ziteng Lu, Jiahao Chang, Xiaoyang Guo, Jiaqing Zhou, Hao Zhao, and Xiaoguang Han. Hi3dgen: High-fidelity 3d geometry generation from images via normal bridging. *arXiv preprint arXiv:2503.22236*, 3:2, 2025. 2, 3
- [54] Biao Zhang, Jiapeng Tang, Matthias Niessner, and Peter Wonka. 3dshape2vecset: A 3d shape representation for neural fields and generative diffusion models. *ACM Transactions On Graphics (TOG)*, 42(4):1–16, 2023. 3
- [55] Longwen Zhang, Ziyu Wang, Qixuan Zhang, Qiwei Qiu, Anqi Pang, Haoran Jiang, Wei Yang, Lan Xu, and Jingyi Yu. Clay: A controllable large-scale generative model for creating high-quality 3d assets. *ACM Transactions on Graphics (TOG)*, 43(4):1–20, 2024. 2, 3
- [56] Longwen Zhang, Qixuan Zhang, Haoran Jiang, YINUO Bai, Wei Yang, Lan Xu, and Jingyi Yu. Bang: Dividing 3d assets via generative exploded dynamics. *ACM Transactions on Graphics (TOG)*, 44(4):1–21, 2025. 2, 3, 5, 6, 7, 1
- [57] Hengshuang Zhao, Li Jiang, Jiaya Jia, Philip HS Torr, and Vladlen Koltun. Point transformer. In *Proceedings of the IEEE/CVF international conference on computer vision*, pages 16259–16268, 2021. 3
- [58] Zibo Zhao, Zeqiang Lai, Qingxiang Lin, Yunfei Zhao, Haolin Liu, Shuhui Yang, Yifei Feng, Mingxin Yang, Sheng Zhang, Xianghui Yang, et al. Hunyuan3d 2.0: Scaling diffusion models for high resolution textured 3d assets generation. *arXiv preprint arXiv:2501.12202*, 2025. 2, 3, 4
- [59] Ziming Zhong, Yanyu Xu, Jing Li, Jiale Xu, Zhengxin Li, Chaohui Yu, and Shenghua Gao. Meshsegmenter: Zero-shot mesh semantic segmentation via texture synthesis. In *European Conference on Computer Vision*, pages 182–199. Springer, 2024. 3

EI-Part: Explode for Completion and Implode for Refinement

Supplementary Material

6. Network Details

FluxDev-1 [18] is employed as the backbone of MVSegNet, while InSegNet adopts the large texturing architecture from UniTex [23].

In the **Explode for Completion** stage, the DiT network utilizes the *Sparse Latent Flow* architecture from Trellis [46], which comprises 24 Transformer blocks. Since we adopt the Flux-Kontext [1] training strategy, a lightweight positional embedding is applied to distinguish noise latent tokens from conditional latent tokens. The resulting embeddings are added to the token features before being input into the DiT blocks.

For the **Implode for Refinement** stage, we utilize the Sparc3D [22] VAE with a latent resolution of 64^3 . To avoid degradation in reconstruction quality, the downsampling operation in the original Stage-II Trellis [46] DiT network is removed, while the internal structure of each DiT block remains unchanged. Positional embeddings are consistently applied to both noise and conditional tokens to encode spatial positional information before being processed by the DiT blocks.

7. Training Details

The training data pairs for the two-stage DiT are constructed as follows:

- **Incomplete part meshes:** These are obtained by first converting the complete mesh into a watertight representation, then discarding the internal structures while preserving the face correspondence information. The resulting meshes are used as the data for incomplete part meshes.
- **Complete part meshes:** These are directly extracted from the original GLB files. Each individual part is processed to ensure watertightness and is then used as the ground-truth (GT) part mesh data.

In the first stage, the VAE is fine-tuned on the curated part dataset, and all mesh data are encoded into the latent space for DiT training. In the second stage, the original Sparc3D [22] VAE is employed to encode meshes into latents, where the latents of incomplete sub-meshes serve as conditions, and the active voxel positions are guided by the GT part meshes.

8. More Comparison

Comparison with Baseline Methods. Fig. 7 presents additional qualitative results compared to state-of-the-art (SOTA) methods. As illustrated, BANG [56] and PartPacker [42] struggle to capture fine geometric details that correspond

with the input model. This issue stems from their practice of embedding all components into a single or dual set of latent tokens, which limits the representational capacity of individual parts and ultimately leads to inaccuracies in geometric detail. HoloPart [51] neglects the interrelationships between parts, leading to unnatural completion outcomes that resemble merely filling a hole, thus compromising structural coherence. While PartCrafter [24] and X-Part [48] utilize a cross-attention mechanism to enhance structural coherence, their reliance on fixed-length part tokens proves inflexible for components of varying sizes. This limitation results in inefficient resource allocation, where larger components may be underrepresented while resources are wasted on smaller parts. OmniPart [52] employs voxel-based representations to adaptively allocate spatial resolution to different parts; however, it supports completion only within active voxels, restricting the available spatial extents for completion. This constraint can lead to implausible part geometries and reduced geometric fidelity. In contrast, our method excels in generating high-quality 3D shapes with well-defined parts, demonstrating significant performance improvements in structural coherence, geometric plausibility, geometric fidelity, and efficiency.

Ablation Study on Explode and Implode. Tab. 2 presents the quantitative comparisons between our method and alternative strategies. Our proposed method outperforms all the other options, achieving the highest scores.

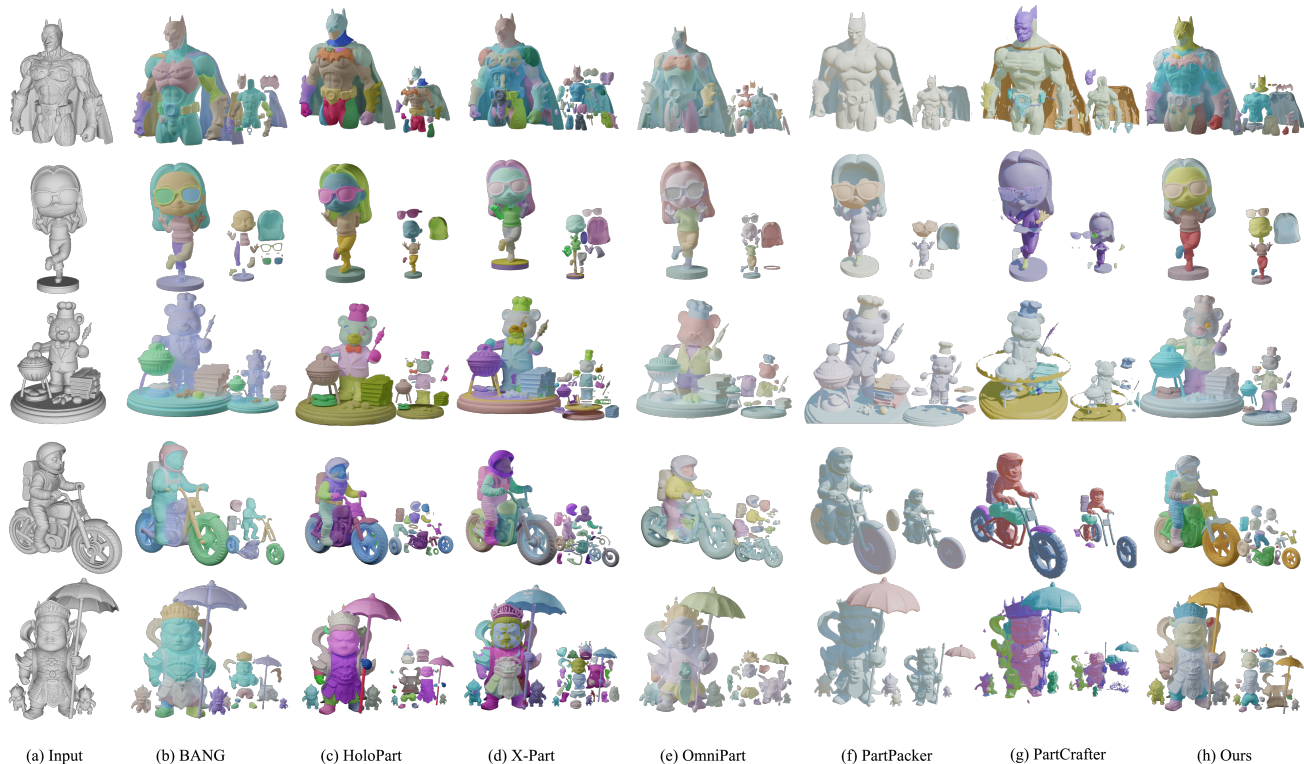


Figure 7. Qualitative comparison between ours and the state of the arts. For each row, the input model (a) is shown alongside the parts generated by (b) BANG [56], (c) HoloPart [51], (d) X-Part [48], (e) OmniPart [52], (f) PartPacker [42], (g) PartCrafter [24], and (h) our method. Our method demonstrates exceptional proficiency in generating high-quality 3D shapes with well-defined parts, achieving significant improvements in structural coherence, geometric plausibility, fidelity, and efficiency.

Table 2. Quantitative comparison across different settings at both the part and overall object levels. Since the part-level ground truth (GT) is derived from the complete results, the absence of the Explode operation results in lower part completion quality, underscoring its significance. Meanwhile, the explode–implode refinement slightly compromises overall mesh accuracy, revealing a trade-off between enhancing part-level details and maintaining global reconstruction precision.

| Setting | Part-level | | | | | | Overall-object | | | | | |
|-------------|----------------------|-----------------|-------------------------------|------------------------|-------------------------|-------------------------|----------------------|-----------------|-------------------------------|------------------------|-------------------------|-------------------------|
| | Voxel IOU \uparrow | CD \downarrow | Voxel F-Score 0.01 \uparrow | F-Score 0.1 \uparrow | F-Score 0.05 \uparrow | F-Score 0.01 \uparrow | Voxel IOU \uparrow | CD \downarrow | Voxel F-Score 0.01 \uparrow | F-Score 0.1 \uparrow | F-Score 0.05 \uparrow | F-Score 0.01 \uparrow |
| w/o Explode | 0.7647 | 0.0153 | 0.8883 | 0.9975 | 0.9866 | 0.7599 | 0.9310 | 0.0092 | 0.9642 | 1.0000 | 1.0000 | 0.9680 |
| w/o Implode | 0.7992 | 0.0168 | 0.8664 | 0.9998 | 0.9937 | 0.8678 | 0.8036 | 0.0171 | 0.8896 | 0.9769 | 0.9615 | 0.8243 |
| Whole | - | - | - | - | - | - | 0.9005 | 0.0152 | 0.9091 | 0.9975 | 0.9869 | 0.8691 |